Molecules and Cells

Morphological Characterization of *small*, *dumpy*, and *long* Phenotypes in *Caenorhabditis elegans*

Joshua Young Cho[1,2,3,4], Tae-Woo Choi[1,2,3,5], Seung Hyun Kim[1,3], Joohong Ahnn[1,2,3,*], and Sun-Kyung Lee[1,2,3,*]

[1]Department of Life Science, School of Natural Sciences, Hanyang University, Seoul 04763, Korea, [2]BK21 PLUS Life Science for BDR Team, Hanyang University, Seoul 04763, Korea, [3]Research Institute for Natural Sciences, Hanyang University, Seoul 04763, Korea, [4]Present address: Doctor of Dental Surgery Program, University of the Pacific, Arthur A. Dugoni School of Dentistry, San Francisco, CA 94103, USA, [5]Present address: Macrogen Inc., Seoul 08511, Korea
*Correspondence: sunkyungl@hanyang.ac.kr (SKL); joohong@hanyang.ac.kr (JA)
https://doi.org/10.14348/molcells.2021.2236
www.molcells.org

The determinant factors of an organism's size during animal development have been explored from various angles but remain partially understood. In *Caenorhabditis elegans*, many genes affecting cuticle structure, cell growth, and proliferation have been identified to regulate the worm's overall morphology, including body size. While various mutations in those genes directly result in changes in the morphological phenotypes, there is still a need for established, clear, and distinct standards to determine the apparent abnormality in a worm's size and shape. In this study, we measured the body length, body width, terminal bulb length, and head size of mutant worms with reported Dumpy (Dpy), Small (Sma) or Long (Lon) phenotypes by plotting and comparing their respective ratios of various parameters. These results show that the Sma phenotypes are proportionally smaller overall with mild stoutness, and Dpy phenotypes are significantly stouter and have disproportionally small head size. This study provides a standard platform for determining morphological phenotypes designating and annotating mutants that exhibit body shape variations, defining the morphological phenotype of previously unexamined mutants.

Keywords: *Caenorhabditis elegans*, dumpy, K-means clustering, long, small

INTRODUCTION

The organismal size is determined by multiple inputs from various biological pathways that affect the size, structure, and organization of the cells comprising the tissues and organs (Bar et al., 2016; Tuck, 2014; Uppaluri et al., 2016). During development, various genetic pathways that regulate cell growth, proliferation, and apoptosis need to be activated appropriately to define the body's dimension and proportion, ultimately determining an individual's body size (Nagashima et al., 2017). Although the regulation of body size by internal and external factors in various organisms has been extensively studied, the genetic pathways contributing to a different aspect of body growth have not been fully identified at the organismal level.

Caenorhabditis elegans, a free-living nematode, is a versatile genetic model system for elucidating genetic pathways that regulate various aspects of organismal growth. *C. elegans* matures to an adult after multiple molting events and having developed distinctive organs that comprise the entire body structures. A genetic screen, which isolates mutant worms with abnormal body size, contributes to identifying several biological pathways that regulate body growth (Brenner, 1974; Savage-Dunn et al., 2003). Several *small* (*sma*) mutant alleles were found to be components of the

Received 1 December, 2020; revised 18 February, 2021; accepted 22 February 2021; published online 10 March, 2021

eISSN: 0219-1032

TGF-β (transforming growth factor-β) pathway, which has been established as one of the primary regulators of body size in worms (Dineen and Gaudet, 2014; Gumienny and Savage-Dunn, 2013). The loss-of-function mutations, such as *lon-1* and *lon-2*, in the negative regulators of TGF-β signaling, results in the *long* (*lon*) phenotype. The body size of those mutants of the TGF-β pathway changes proportionally, suggesting that TGF-β signaling plays a crucial role in coordinating organisms' growth (Harada et al., 2016).

In contrast, *dumpy* (*dpy*) mutants exhibit a disproportionate reduction in body size, often with a thicker middle body and a shorter length. Many *dumpy* mutant alleles are in genes encoding collagens, the cuticle's significant components, or an exoskeleton, enclosing the entire worm (Page and Johnstone, 2007). The analysis of one *long* mutant cuticle collagen allele, *lon-3*, indicates that proper assembly of an organism's external structure is necessary to build a standard body shape.

Analyzing the characteristics of body shape phenotypes in various mutants, such as Dpy, Sma, and Lon, will be essential for investigating the role of genetic pathways in body growth. However, due to the differential gene expression in different body parts, there is a significant challenge in analyzing body size and shape to determine the phenotype accurately. In the currently available open-source databases, some strains are often reported as both Dpy and Sma, bringing confusion to morphological concepts and phenotype designations (WormBase; https://wormbase.org/). But, at the same time, these records suggest that there may be a growth-regulating gene in complex networks of pathways differentially regulating body shape and size and contributing to organismal growth. Thus, the question of how a gene regulating body size plays a role in constructing an organismal body with optimal size and shape remains unanswered.

In this study, we determined the morphological phenotype, in terms of body size, of 46 strains of *C. elegans* based on their respective body length, body width, pharynx length, and head size. Among them, 41 strains have been previously reported to have the Dpy, Sma, or Lon, according to the WormBase and published literature. We analyzed the worms' body size and evaluated each parameter's ratios, such as the overall head shape, body length, body width, pharynx length, and head size, of each strain to detect previously unknown differences in body morphology. Utilizing this analysis, we found that the ratio of body length to body width and the ratio of head size to pharynx length can be useful parameters to identify a worm's morphology. We validated the previously reported phenotypes of 37 mutants. We reassigned *unc-32(e189)* as Sma, but not Dpy that used to be confusingly annotated. We also assigned morphological phenotypes for 2 mutants, previously never characterized as abnormal body phenotype: *osm-5(p813)* and *unc-4(gk668)*, small and long, respectively. The approach employed in this study provides a simple but useful method to define the morphological phenotypes associated with body size, excavating novel genes that possibly regulate organismal growth.

MATERIALS AND METHODS

Strains and maintenance

Worms were grown at 20°C according to the standard protocol (Brenner, 1974). The wild-type N2 animals and the following strains used in this study were obtained from the *C. elegans* Genetics Center funded by National Institutes of Health (NIH) office of Research Infrastructure Programs (P40 OD010440) or National Bioresource Project Japan, and some strains are generated by the *C. elegans* Reverse Genetics Facility at the University of British Columbia, which is part of the international *C. elegans* Gene Knockout Consortium (C. elegans Deletion Mutant Consortium, 2012) : *bli-3(e767), calu-1(tm1783), dpy-1(e1), dpy-10 (e128), dpy-11(e224), dpy-13(e184), dpy-17(e164), dpy-4(e1166), dpy-5(e907), dpy-7(e88), hnd-1(q740), unc-104(e1265), unc-120(st365), unc-76(e911), bli-2(e768), egl-30(n686), egl-36(n728), hsf-1(sy441), tax-6(ok2065), unc-13(e1091), unc-11(e47), unc-22(e66), unc-32(e189), unc-68(e587), lon-1(e185), lon-2(e678), lon-3(e2175), sqt-3(e24), sup-9(n180), ser-1(ok345), mod-1(ok103), egl-4(n478), dpy-14(e188), dpy-8(e130), sma-1(ru18), sma-3(e491), sma-6(e1482), unc-32(e189), che-2(e1033), osm-3(p802), osm-5(p813), osm-6(p811), unc-4(e120), unc-4(e2309), unc-4(gk668), unc-4(gk705)*, and *unc-4(wd44)* (Supplementary Table S1).

Measurements of body length, body width, pharynx length, and head size

L4 larvae were picked to fresh plates and incubated at 20°C for 24 h to measure the body sizes of adults (Fig. 1). L4 larvae worms with an apparent white crescent surrounding the visible prospective vulva were chosen. One-day adult worms were mounted on a 2% agarose pad, paralyzed with 10 mM levamisole (L9756; Sigma-Aldrich, USA), and imaged under 100× with Zeiss AxioCam using the Normarski optics and an attached AxioCam digital camera. All measurements were performed with AxioVs40 V 4.8.2.0 (Carl Zeiss, Germany).

K-means clustering

We compared the ratio of body length to body width to the ratio of head size to pharynx length to further quantify the parameters of the worm's morphology. We applied the k-means clustering approach with the Euclidean distance (ED) to measure for similarity. Then, we analyzed 4 formed clusters of wildtype, dumpy, small, and long, to study the existing phenotypic characteristics of the worm's morphology.

Measuring the distance between data points and cluster centroids was the fundamental first step for all clustering methods. The algorithm used in clustering was the objective function given by:

$$J(V) = \sum_{i=1}^{n} \sum_{j=1}^{k} (\| x_i - v_j \|)^2$$

where $\|x_i - v_j\|^2$ is the ED between a data point x_i and its respective cluster center v_j.

Data points are in the space represented by the objects that are being clustered. These points represent initial group centroids in which each object is assigned to the group that has the closest centroid according to the formula given by:

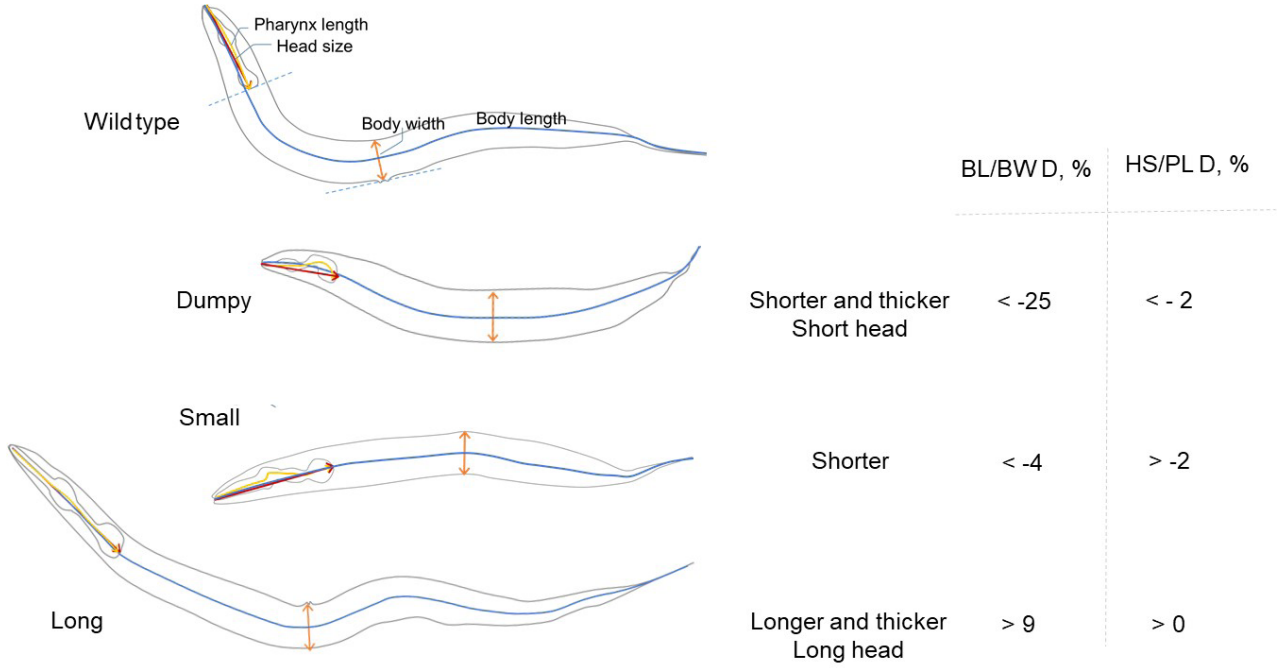

Fig. 1. Measurement of the body size. Body length (BL) was measured from the nose to the tail tip, following the worm's centerline (blue). Body width (BW) was measured at the position of the vulva, perpendicular to the line at the vulva (orange). Head size (HS) was measured as the direct distance from the nose to the terminal bulb's posterior end (red). Pharynx length (PL) was measured by tracing the centerline from the buccal cavity to the terminal bulb's posterior end (yellow). BL/BW and HS/PL differences (BL/BW D and HS/PL D) were calculated as percentages of BL/BW and HS/PL of wild type N2. Each phenotype of dumpy, small, and long is characterized according to the values of BL/BW D and HS/PL D determined in this study (see below and Fig. 5). Dumpy is described as 'shorter and thicker', small is 'shorter', and long, 'longer and thicker'.

$$v_i = (\frac{1}{k})\sum_{j=1}^{k} x_i$$

where k represents the number of data points in i^{th} cluster.

All objects were reassigned when the number of cluster centers was manually inputted as three. The calculation of the positions of the K centroids was repeated until the centroids became constant. Wolfram Mathematica and R were used to compute the *k*-means clustering algorithm and ED values.

RESULTS

Body size analysis of morphological mutants

Organismal morphology is determined by various genetic pathways; however, it remains unclear how these genetic pathways play a role in defining certain characteristics of body size and morphology. We investigated the body morphology of mutants with previously reported defects in body size. First, we chose a group of diverse strains, such as *dpy* (*dumpy*), *sma* (*small*), and *lon* (*long*) (Supplementary Table S1, Fig. 2A). The previously categorized *dpy* mutants include *bli-3(e767)*, *calu-1(tm1783)*, *dpy-1(e1)*, *dpy-10(e128)*, *dpy-11(e224)*, *dpy-13(e184)*, *dpy-17(e164)*, *dpy-4(e1166)*, *dpy-5(e907)*, *dpy-7(e88)*, *hnd-1(q740)*, *unc-104(e1265)*, *unc-120(st365)*, and *unc-76(e911)*. The previously categorized *sma* mutants include *bli-2(e768)*, *egl-30(n686)*, *egl-36(n728)*, *hsf-1(sy441)*, *tax-6(ok2065)*, *unc-13(e1091)*, *unc-11(e47)*, *unc-22(e66)*, *unc-32(e189)*, and *unc-68(e587)*. The previously categorized *lon* mutants include *lon-1(e185)*, *lon-2(e678)*, *lon-3(e2175)*, *sqt-3(e24)*, *sup-9(n180)*, *ser-1(ok345)*, *mod-1(ok103)*, and *egl-4(n478)*. Different studies have reported *dpy-14(e188)*, *dpy-8(e130)*, *sma-1(ru18)*, *sma-3(e491)*, *sma-6(e1482)*, and *unc-32(e189)* to be either *dpy* or *sma*.

When the worms were measured 24 h after the L4 larval stage, the average body length of the reportedly *dpy* mutants was 29.27% shorter than that of the N2 wild type (Figs. 1 and 2B). Similarly, the average body length of the reportedly *sma* mutants was 13.87% shorter than that of the wild type. In contrast, the average body length of the reportedly *lon* mutants was 43.56% longer than that of the wild type. These results were consistent with the previous observation that both *dpy* and *sma* mutants were shorter, while *lon* mutants were longer than the wild-type animals (Brenner, 1974).

We also measured the body width of these mutants (Fig. 1). The reportedly dpy and lon mutants' average body width was 10.78% and 8.97%, respectively, greater than that of the wild type (Fig. 2C). The average body width of the reportedly *sma* mutants was similar to that of the wild type. These data indicate that *dpy* mutants are shorter and thicker, *lon*

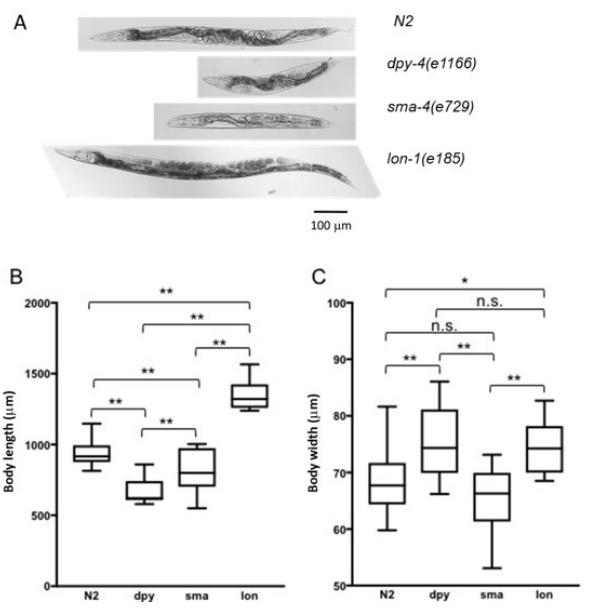

Fig. 2. The body length and body width of the N2 wild type and mutants with reported Dpy, Sma, or Lon phenotypes. All measurements were taken at the 1-day adult stage. (A) Nomarski differential interference contrast (DIC) images of the *dpy-4(e1166)*, *sma-4(e729)*, and *lon-1(e185)* mutants and the wild type (N2). (B) The average body length of N2 compared to that in the mutants with reported Dpy, Sma, and Lon phenotypes. (C) The average body width of N2 compared to that in the mutants with reported Dpy, Sma, or Lon phenotypes. The number of animals measured was 36 for N2, or 21 to 37 for each mutant type. n.s., no significance. $*P < 0.05$, $**P < 0.01$ (ANOVA with Bonferroni test).

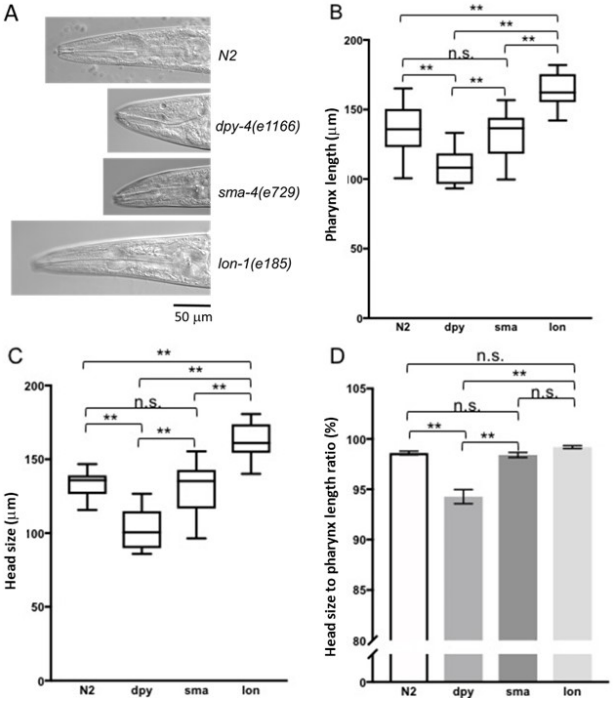

Fig. 3. The pharynx length and head size of N2 wild type and mutants with reported Dpy, Sma, or Lon phenotypes. All measurements were taken at the 1-day adult stage. (A) Nomarski differential interference contrast (DIC) images of the pharynx and head region of the *dpy-4(e1166)*, *sma-4(e729)*, and *lon-1(e185)* mutants and the wild type (N2). (B) The average pharynx length of N2 compared to that in the mutants with reported Dpy, Sma, or Lon phenotypes. (C) The average head size of the wild type compared to that in the mutants with reported Dpy, Sma, or Lon phenotypes. The number of animals measured was 36 for N2, or 21 to 37 for each mutant type. n.s., no significance. $**P < 0.01$ (ANOVA with Bonferroni test).

mutants are thicker and longer, and *sma* mutants are neither thicker nor thinner but shorter than the wild-type animals. The *sma* mutants were previously reported to be an accurately scaled-down form of the *N2* wild type animals (Brenner, 1974). However, our findings show that the average body width of the reportedly *sma* mutants was not significantly different from that of the wild type. The result suggests that the average morphology of the previously defined *sma* mutants was likely disproportionate. We also suspected that the group of *sma* mutants we investigated may include some mutants that are not actually *small* and could alter the average measurements.

Some *dpy* mutants are defective in cuticle development, and their bodies are often squeezed in a small, underdeveloped cuticle cavity (Page and Johnstone, 2007). The malformed cuticle sometimes results in a winding pharynx in a small head (Avery and Shtonda, 2003; Ferrier et al., 2011). Therefore, we examined the pharynx further to characterize the body morphology (Fig. 3A). At 24 h after the L4 larval stage, the pharynx length of the *dpy* mutants was 19.88% shorter than that of the wild type (Fig. 3B). Surprisingly, in contrary to a previous report in which the pharynx length of the *sma* mutants was shorter than that of the wild type (Dineen and Gaudet, 2014), the pharynx length of the *sma* mutants was not significantly different from that of the wild type. On the other hand, the pharynx length of the *lon* mutants was 25.08% longer than that of the wild type. While measuring, we found that the pharynx of the *dpy* mutants showed a deformation with a pharynx that was crooked from the procorpus to the terminal bulb (Fig. 3A). Based on this observation, we hypothesized that a small head could not allow the pharynx to develop in full size.

We then measured the head size and found that the average head size of the *dpy* mutants was 22.46% smaller than that of the wild type. However, the head size of the *sma* mutants showed no significant difference from that of the wild type. The average head size of *lon* mutants was 22.12% longer than that of the wild type (Fig. 3C). The ratio of head size to pharynx length of N2, Sma, and Lon phenotypes were all close to 1 (Fig. 3D). However, the ratio of head size to pharynx length of the Dpy phenotype was significantly smaller than that of the wild type, suggesting a disproportionate reduction in the head of the *dpy* mutants may be responsible for the deformation of the pharynx.

Establishment of standards to define morphological phenotypes

The analysis of body morphology suggests that previous phenotyping may not reflect the actual, i.e., proportionate morphology. We visualized individual mutants' morphological phenotype by plotting each worm's body size relative to the wild type by integrating four parameters: body length, body width, pharynx length, and head size (Figs. 4 and 5). Our k-means clustering centroids indicate that the average body lengths of the *dpy*, *sma*, and *lon* mutants are 676.49 μm, 810 μm, and 1,350 μm, respectively. The average body widths of the *dpy*, *sma*, and *lon* mutants are 74.52 μm, 65.42 μm, and 74.67 μm, respectively. The average head sizes of the *dpy*, *sma*, and *lon* mutants are 102.32 μm, 130.50 μm, and 162.06 μm, respectively. Lastly, the average pharynx length of the *dpy*, *sma*, and *lon* mutants are 108.73 μm, 132.55 μm, and 163.37 μm, respectively.

Mutants that belong to their respective morphological phenotype tend to cluster at a specific region of the graph (Fig. 5). The mutants with a defect in a cuticle collagen protein, *dpy-1(e1), dpy-4(e1166), dpy-5(e907), dpy-8(e130), dpy-10(e128), dpy-11(e224), dpy-13(e184), dpy-14(e188),* and *dpy-17(e164),* were clustered in a region where the ratio of body length to body width was at least 25% less than that of the wild type, and the ratio of head size to pharynx length was below 2% compared to the wild type (Figs. 4 and 5).

dpy-7(e88) was the only cuticle collagen mutant that fell out of the *dpy* cluster. While its ratio of body length to body width was reduced by the same degree as other Dpy phenotypes, its ratio of head size to pharynx length was reduced by 38%, indicating a proportional pharynx length relative to its head size. DPY-7 is spatially restricted to the transverse grooves or furrows of the cuticle cortex called the annulations or annular furrows (Thein et al., 2003). DPY-7 is similar in structure to other *C. elegans* collagen proteins but does not fit perfectly into any of the previously described classes because of its differences in the lengths of the Gly – X – Y repeats and positions of cysteine residues (Johnstone et al., 1992). The DPY-7 encoded by the *dpy-7(e88)* allele has a glycine-to-arginine substitution at residue 156, suggesting a disruption in the formation of a triple helix with two other collagen helices. However, this alteration in DPY-7 specific to the annular furrows may not result in cuticle shrinkage in the head region or reduced head size.

The plotting revealed that *unc-32(e189)* would be small rather than dumpy (Fig. 5). *unc-32(e189)* is previously reported as either small or dumpy (Shephard et al., 2011; WormBase). *unc-32* encodes V-type ATPase V_O subunit a and its human orthologs are implicated in many diseases including cutis laxa and osteopetrosis, both of which result in stunted growth and deformity (Lee et al., 2010).

In the plotting, we also included several mutants' data points to try to determine their morphology, which had never been reported. Among them, *osm-5(p813)* is clustered in the group of *small*, whereas *unc-4(gk668)* is in that of *long*. *osm-5* is an ortholog of mammalian intraflagellar transport 88 (IFT88) that functions in non-motile cilium biogenesis and crucial in craniofacial development. *osm-5(p813)* exhibits impaired cilium assembly of sensillum, and the defective head structure consequently contributes to moderately retarded growth (Qin et al., 2001). *unc-4* encodes a transcription factor that functions in neural wiring and its mammalian ortholog is involved in neurogenesis and somitogenesis (Sammeta et al., 2010; Sewell et al., 2009; Skuntz et al., 2009). *unc-*

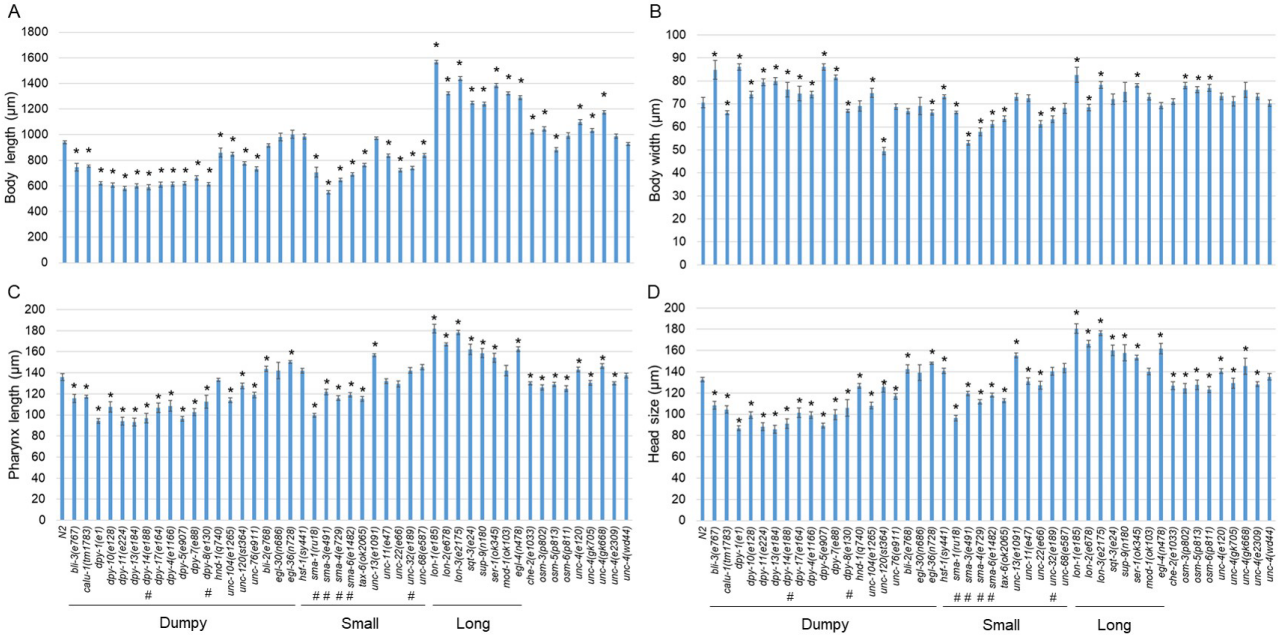

Fig. 4. Body sizes of individual mutants with reported dpy, sma, and lon phenotypes. All measurements were taken 24 h after L4 pick. #, mutants reported as having both dpy and sma phenotypes. (A) Body length. (B) Body width. (C) Pharynx length. (D) Head size. The number of animals measured was 36 for N2, or 21 to 37 for each mutant type. $*P < 0.05$ compared to the wild-type (Student *t*-test).

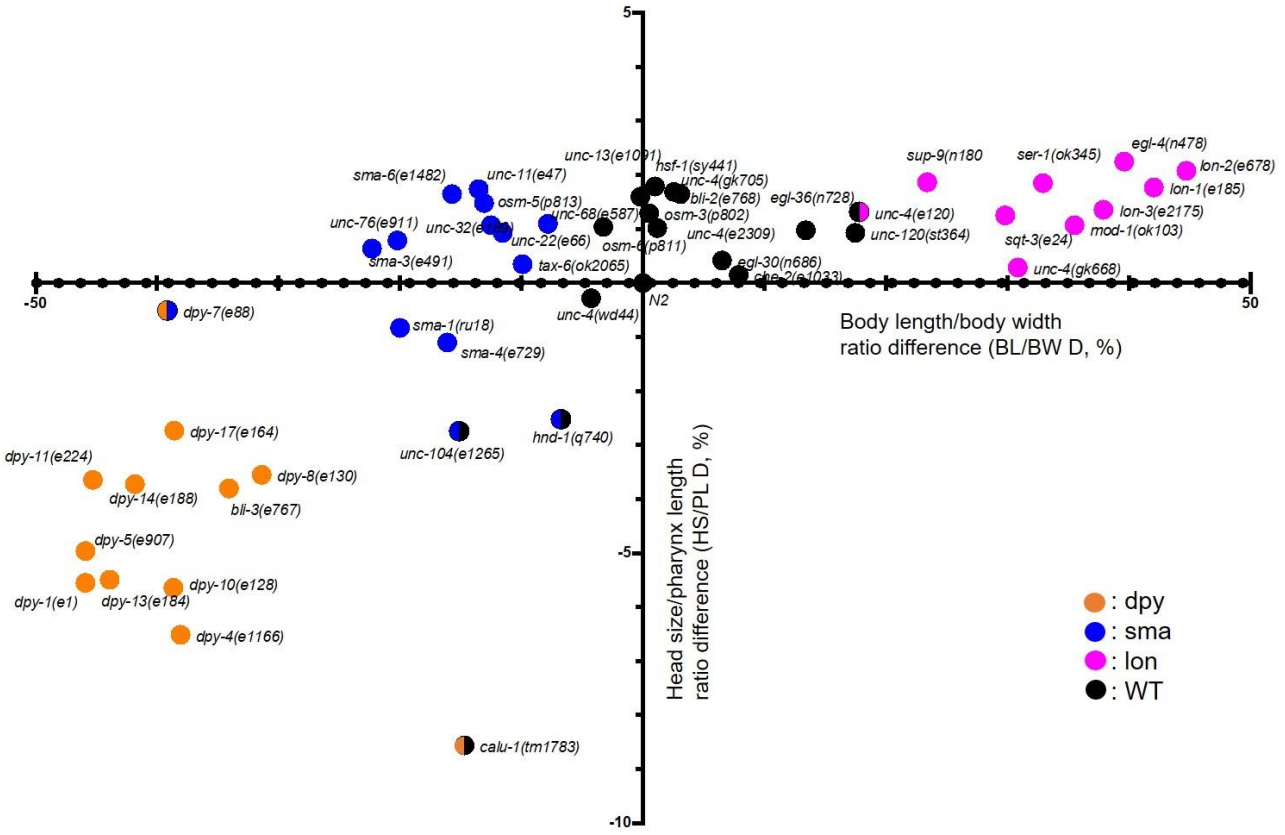

Fig. 5. The illustration of the mutant phenotypes relative to the wild-type phenotype. The differences (%) in the ratio of body length to body width (BL/BW D, x-axis) and the ratio of head size to pharynx length (HS/PL D, y-axis) were plotted relative to the wild type located at (0,0). K-clustering generates four clusters of *dumpy* (dpy; orange), *small* (sma; blue), *long* (lon; magenta), and wild type (WT; black), and mild phenotype (shaded in semi-circles) is also indicated. *Dumpy* is characterized in case BL/BW D is less than -25% and HS/PL D is less than -2%, small is in case BL/BW D is less than -4% and HS/PL D is more than -2%, and long, BL/BW D is more than 9% and HS/PL D is more than 0% (also see Fig. 1).

4(gk668) exhibited uncoordinated motility that is a phenotype widely reported in other mutant alleles of *unc-4* tested together, but was solely clustered as *long*. *unc-4(gk668)* contains 1.6 kb deletion spanning a part of the coding region and downstream untranslated region. The deletion mutation may cause further dysregulation of other associated genes that result in the morphological difference. Both *osm-5* and *unc-4* are critical in nerve system development, and numerous genes functioning in neurons are implicated in body size controls. For example, *tax-6* loss-of-function mutants are *small,* and its activity in neurons is responsible for standard body size (Kuhara et al., 2002; Li et al., 2015). Serotonin signaling in specific neurons controls body size, and serotonin receptor mutants of *ser-1(ok345)* and *mod-1(ok103)* are grouped in *long* cluster (Fig. 5). Therefore, the clustering analysis provides a practical primary analysis tool to assign body size phenotypes.

DISCUSSION

Morphological analysis of mutant *C. elegans* has been broadly utilized to investigate the function of genes. The phenotypes, such as Sma, Dpy, and Lon, are commonly used to study body size. The analysis of body size has been useful in defining distinct morphological phenotypes. However, the research is mainly dependent on empirical observation, often accompanied by a simple body length measurement.

Here, we demonstrate a novel method of categorizing morphological phenotypes of Dpy, Sma, and Lon with multiple body parameters. We analyze 46 mutant worms' body size by measuring their body length, body width, pharynx length, and head size. We evaluated the ratios between each parameter to detect the relatively subtle differences in body morphology and head shape. We also validated some previously reported phenotypes with reassignments and provided the optimal parameters to identify a worm's phenotype.

WormBase has served as a database for in-depth phenotypic and genetic information of *C. elegans*. WormBase receives phenotype information from the direct submissions by primary literature, individual researchers, and gene knockout consortiums. The vocabulary used to describe similar or identical phenotypes and the level of precision in the descriptions often vary between these sources. Consequently, different words were used to annotate the same phenotypes. Also,

there was no inherent hierarchical organization in the descriptions, making the retrieval of phenotypic information via searches more cumbersome. As a result, there is significant difficulty defining a worm's phenotype, thus interfering with the useful comparisons between strains.

Extensive phenotyping requires measuring many parameters that quantify body size and organ length and calculate the ratios between different parameters. While mutations that affect cuticle collagen are often responsible for the Dpy phenotype, several major pathways involving TGF-β, spectrin, calcineurin, and feeding efficiency determine the body size phenotypes (Mörck and Pilon, 2006). Though the smaller body size of *C. elegans* mutants has been recognized as an obvious developmental defective phenotype, clear and distinct standards have not been established to indicate a wild-type worm's apparent size and shape. Our analyses suggest that the Sma phenotype involves a proportionally smaller size with mild stoutness, and the Dpy phenotype involves a significant increase in stoutness and a disproportionally small head size harboring a winding pharynx. This study utilized K-means clustering, which aims to partition data points into *k* number of clusters. Each data point belongs to the cluster with the nearest mean represented as a cluster centroid, which serves as a prototype of the cluster (Lloyd, 1982). Although cluster shapes and centroids can change as more data points are included, the algorithm provides practical insight grouping individual data points into classified types. K-means clustering can be further utilized in future research to better understand the specific morphological characteristics of a phenotype. Additional parameters such as egg and larvae size, volume and locomotion can also enhance the phenotypic descriptions (Chung et al., 2020; Levine and Lee, 2020; Yemini et al., 2013). More extensive analyses dealing with many strains may lead to the formation of subgroups within a particular phenotype.

Note: Supplementary information is available on the Molecules and Cells website (www.molcells.org).

ACKNOWLEDGMENTS

Some strains are provided by the CGC, funded by NIH Office of Research Infrastructure Programs (P40 OD010440) or National Bioresource Project Japan. This research was supported by the Basic Science Research Program through the National Research Foundation of Korea (NRF) funded by the Ministry of Education, Science and Technology (2018R1A2A3074987 to S.K.L.; 2018R1D1A1B07046893 to J.A.) and Research Grant from Hanyang University (201500000001686).

AUTHOR CONTRIBUTIONS

J.Y.C., T.W.C., and S.H.K. performed experiments and collected data. J.Y.C. and S.K.L. analyzed data and generated figures. J.Y.C., S.K.L., and J.A. wrote the manuscript. S.K.L. and J.A. designed the study and secured funding.

CONFLICT OF INTEREST

The authors have no potential conflicts of interest to disclose.

ORCID

Joshua Young Cho https://orcid.org/0000-0002-9379-3745
Tae-Woo Choi https://orcid.org/0000-0002-3329-6923
Seung Hyun Kim https://orcid.org/0000-0003-1140-410X
Joohong Ahnn https://orcid.org/0000-0003-2229-3580
Sun-Kyung Lee https://orcid.org/0000-0001-5368-0722

REFERENCES

Avery, L. and Shtonda, B.B. (2003). Food transport in the C. elegans pharynx. J. Exp. Biol. *206*, 2441-2457.

Bar, D.Z., Charar, C., Dorfman, J., Yadid, T., Tafforeau, L., Lafontaine, D.L.J., and Gruenbaum, Y. (2016). Cell size and fat content of dietary-restricted Caenorhabditis elegans are regulated by ATX-2, an mTOR repressor. Proc. Natl. Acad. Sci. U. S. A. *113*, E4620-E4629.

Brenner, S. (1974). The genetics of Caenorhabditis elegans. Genetics *77*, 71-94.

C. elegans Deletion Mutant Consortium. (2012). Large-scale screening for targeted knockouts in the Caenorhabditis elegans genome. G3 (Bethesda) *2*, 1415-1425.

Chung, K.W., Kim, J.S., and Lee, K.S. (2020). A database of Caenorhabditis elegans locomotion and body posture phenotypes for the peripheral neuropathy model. Mol. Cells *43*, 880-888.

Dineen, A. and Gaudet, J. (2014). TGF-β signaling can act from multiple tissues to regulate C. elegans body size. BMC Dev. Biol. *14*, 43.

Ferrier, A., Charron, A., Sadozai, Y., Switaj, L., Szutenbach, A., and Smith, P.A. (2011). Multiple phenotypes resulting from a mutagenesis screen for pharynx muscle mutations in Caenorhabditis elegans. PLoS One *6*, e26594.

Gumienny, T.L. and Savage-Dunn, C. (2013). TGF-β signaling in C. elegans. In WormBook, The C. elegans Research Community, ed. (Pasadena, CA: WormBook), https://doi.org/10.1895/wormbook.1.22.2

Harada, S., Hashizume, T., Nemoto, K., Shao, Z., Higashitani, N., Etheridge, T., Szewczyk, N.J., Fukui, K., Higashibata, A., and Higashitani, A. (2016). Fluid dynamics alter Caenorhabditis elegans body length via TGF-β/DBL-1 neuromuscular signaling. NPJ Microgravity *2*, 16006.

Johnstone, I.L., Shafi, Y., and Barry, J.D. (1992). Molecular analysis of mutations in the Caenorhabditis elegans collagen gene dpy-7. EMBO J. *11*, 3857-3863.

Kuhara, A., Inada, H., Katsura, I., and Mori, I. (2002). Negative regulation and gain control of sensory neurons by the C. elegans calcineurin TAX-6. Neuron *33*, 751-763.

Lee, S.K., Li, W., Ryu, S.E., Rhim, T., and Ahnn, J. (2010). Vacuolar (H+)-ATPases in Caenorhabditis elegans: what can we learn about giant H+ pumps from tiny worms? Biochim. Biophys. Acta *1797*, 1687-1695.

Levine, E. and Lee, K.S. (2020). Microfluidic approaches for Caenorhabditis elegans research. Anim. Cells Syst. (Seoul) *24*, 311-320.

Li, W., Bell, H.W., Ahnn, J., and Lee, S.K. (2015). Regulator of calcineurin (RCAN-1) regulates thermotaxis behavior in Caenorhabditis elegans. J. Mol. Biol. *427*, 3457-3468.

Lloyd, S. (1982). Least squares quantization in PCM. IEEE Trans. Inf. Theory *28*, 129-137.

Mörck, C. and Pilon, M. (2006). C. elegans feeding defective mutants have shorter body lengths and increased autophagy. BMC Dev. Biol. *6*, 39.

Nagashima, T., Ishiura, S., and Suo, S. (2017). Regulation of body size in Caenorhabditis elegans: effects of environmental factors and the nervous system. Int. J. Dev. Biol. *61*, 367-374.

Page, A.P. and Johnstone, I.L. (2007). The cuticle. In Wormbook, The C. elegans Research Community, ed. (Pasadena, CA: WormBook), https://doi.org/10.1895/wormbook.1.138.1

Qin, H., Rosenbaum, J.L., and Barr, M.M. (2001). An autosomal recessive polycystic kidney disease gene homolog is involved in intraflagellar transport in C. elegans ciliated sensory neurons. Curr. Biol. *11*, 457-461.

Sammeta, N., Hardin, D.L., and McClintock, T.S. (2010). Uncx regulates proliferation of neural progenitor cells and neuronal survival in the olfactory epithelium. Mol. Cell. Neurosci. *45*, 398-407.

Savage-Dunn, C., Maduzia, L.L., Zimmerman, C.M., Roberts, A.F., Cohen, S., Tokarz, R., and Padgett, R.W. (2003). Genetic screen for small body size mutants in C. elegans reveals many TGFbeta pathway components. Genesis *35*, 239-247.

Sewell, W., Sparrow, D.B., Smith, A.J., Gonzalez, D.M., Rappaport, E.F., Dunwoodie, S.L., and Kusumi, K. (2009). Cyclical expression of the Notch/Wnt regulator Nrarp requires modulation by Dll3 in somitogenesis. Dev. Biol. *329*, 400-409.

Shephard, F., Adenle, A.A., Jacobson, L.A., and Szewczyk, N.J. (2011). Identification and functional clustering of genes regulating muscle protein degradation from amongst the known C. elegans muscle mutants. PLoS One *6*, e24686.

Skuntz, S., Mankoo, B., Nguyen, M.T., Hustert, E., Nakayama, A., Tournier-Lasserve, E., Wright, C.V., Pachnis, V., Bharti, K., and Arnheiter, H. (2009). Lack of the mesodermal homeodomain protein MEOX1 disrupts sclerotome polarity and leads to a remodeling of the cranio-cervical joints of the axial skeleton. Dev. Biol. *332*, 383-395.

Thein, M.C., McCormack, G., Winter, A.D., Johnstone, I.L., Shoemaker, C.B., and Page, A.P. (2003). Caenorhabditis elegans exoskeleton collagen COL-19: an adult-specific marker for collagen modification and assembly, and the analysis of organismal morphology. Dev. Dyn. *226*, 523-539.

Tuck, S. (2014). The control of cell growth and body size in Caenorhabditis elegans. Exp. Cell Res. *321*, 71-76.

Uppaluri, S., Weber, S.C., and Brangwynne, C.P. (2016). Hierarchical size scaling during multicellular growth and development. Cell Rep. *17*, 345-352.

Yemini, E., Jucikas, T., Grundy, L.J., Brown, A.E.X., and Schafer, W.R. (2013). A database of Caenorhabditis elegans behavioral phenotypes. Nat. Methods *10*, 877-879.